Ion-beam modification of fullerene

S. Prawer and K. W. Nugent
School of Physics, University of Melbourne, Parkville, Victoria 3052, Australia

S. Biggs
School of Chemistry, University of Melbourne, Parkville, Victoria 3052, Australia

D. G. McCulloch
Electron Microscope Unit, University of Sydney, NSW 2006, Australia

W. H. Leong
School of Chemical and Biological Sciences, Deakin University, Geelong 3217, Australia

A. Hoffman and R. Kalish
Solid State Institute, Technion-Israel Institute of Technology, Haifa, 32000, Israel

The response of thin films of fullerene (C_{60}) to energetic ion impact is investigated. The diagnostics employed include Fourier-transform infrared and Raman spectroscopies, cross-sectional transmission electron microscopy, and atomic force microscopy. By combining the information obtained from these diagnostics with that from the dependence of the conductivity on ion dose, it is concluded that each C_{60} molecule completely disintegrates when hit by an energetic ion. The cross section for the destruction is about 6×10^{-13} cm^2 for irradiation with 620-keV Xe ions. The disintegration occurs when C atoms are knocked out of the molecule either directly by the impinging ion or by an energetic knock-on C atom within the damage cascade. This process is quite different from the Coulomb-explosion mechanism previously proposed in the literature. For very low ion doses ($< 1 \times 10^{11}$ Xe/cm^2) most of the C_{60} molecules remain intact; however this dose is sufficient to completely disrupt the ordering of the C_{60} molecules in the van der Waals bonded C_{60} solid. Disruption of the lattice ordering at such low doses is considered to be attributable to the weakness of the van der Waals forces which bind the C_{60} clusters together into the molecular solid.

INTRODUCTION

The discovery of the existence of carbon in the form of large molecules which contain some "magic numbers" of carbon atoms[1] and the ability to dope these materials with alkali metals to produce superconducting properties[2] are among the more important recent findings in solid-state physics. The most abundant of these molecular clusters is C_{60}, often referred to as fullerene. It has a closed "soccer-ball"-type structure similar to a geodesic dome comprised of 20 hexagons and 12 pentagons in which each atom is sp^2 bonded to its neighbor, leaving one electron per carbon atom for conduction. However, in the solid form (single crystal or amorphous) the C_{60} clusters are well separated and are only weakly bonded to each other by van der Waals forces. Hence, as a consequence, despite the presence of sp^2 bonding, the material as a whole is electrically insulating.[2] When crystallized, fullerene displays a cubic structure with a lattice constant of 1.417 nm, a C_{60}-C_{60} nearest-neighbor distance of 1.002 nm and a density of 1.72 g/cm^3.[3]

When alkali-metal dopants are introduced into the fullerene structure either during deposition or by postdeposition intercalation they occupy interstitial sites which re-

sults not only in a conducting form of C_{60} but also in superconducting behavior with, for example, $T_c = 18$ K for K_3C_{60}.[2] One method for the nonequilibrium introduction of dopant atoms into solids is ion implantation. This method circumvents the limitations of solid solubility and offers accurate control of dopant concentration and profile. However, ion implantation is always accompanied by damage to the target, and may overshadow the electrical modification induced by the presence of the dopant. Hence it is important that damage effects be properly understood. Previous work[4] attempting to dope C_{60} by K ion implantation may not have fully taken into account the effect of ion-beam damage on the electrical properties of the fullerene films.

The response of C_{60} to ion impact has recently been investigated for the case of proton[5] and heavy (Xe) ion irradiation.[6] For the former, Fourier-transform infrared (FTIR) spectroscopy, x-ray fluorescence and glancing angle x-ray-diffraction techniques were used to study the effects of high dose (up to 1×10^{16} H/cm^2) 200-keV proton irradiation of C_{60} films. The FTIR signal of C_{60} was found to decrease without significant changes to either the peak position or peak width. Based on this evidence, and on the exponential decay of the FTIR peak intensity, the authors of Ref. 5 concluded that each C_{60} molecular

cluster is destroyed in a Coulomb explosion induced by the passage of the proton due to the disruption of its electronic structure.

An alternative approach to the investigation of the response of C_{60} to heavy-ion beam damage has recently been published by us.[6] In that work, the changes in resistivity of fullerene (C_{60}) films subjected to 320-keV Xe ion irradiation were investigated as a function of ion dose. From a comparison of this dependence with similar data on Xe irradiated diamond and with data on C implanted fused quartz, it was concluded that upon ion impact C_{60} clusters completely disintegrate. The conclusion was reached because it was found that the size of the conducting centers between which hopping conduction occurs is that of a single C atom. In addition the induced conductivity was found to be consistent with the proposition that, upon ion impact, each C_{60} releases 60 carbon atoms which disperse amongst the remaining intact C_{60} spheres giving rise to hopping conductivity between isolated C atoms.

The major differences between the two above studies lie both in the physical quantities measured and in the interpretation of the data. The FTIR technique employed in Ref. 5 is primarily sensitive to the remaining intact C_{60} spheres after ion irradiation. From the *decrease* in the FTIR peak intensity as a function of ion dose the authors were able to deduce an effective cross section for C_{60} destruction which was found to be about 6×10^{-17} cm^2. By contrast, in the work of Ref. 6 the measurement of the *increase* of the electrical conductivity with increasing dose is primarily sensitive to the presence of conducting species in the film, i.e., to the *remnants* of the C_{60} disintegration. These were found to be predominantly isolated C atoms.

Although both studies conclude that ion impact leads to disintegration of C_{60}, the physical processes involved are not yet clear. In the FTIR study,[5] the authors propose that the mechanism for the disintegration involves the ionization of the entire C_{60} molecule leading to large repulsive forces followed by a Coulomb explosion. If correct, this process should depend on the energy lost by the protons via the electronic slowing down process, and should therefore scale with $(dE/dx)_{electronic}$. In contrast, based on energy deposition arguments, it has been proposed in Ref. 6 that the explosion of C_{60} is caused by the destabilization of the C_{60} structure as a result of the direct knockout of one (or more) C atoms. This process should depend on the energy lost by the ion via the nuclear slowing down process and hence should depend on $(dE/dx)_{nuclear}$.

In the present work we attempt to illuminate the question of the nature of the interaction between energetic heavy ions and fullerene films. We search for possible fullerene fragments resulting from the ion-beam interaction. A wide variety of experimental techniques are employed to study the response of the C_{60} films to different doses of 620-keV Xe ion implantation. FTIR and Raman spectroscopies are used to search for fragments and to deduce the cross section for C_{60} destruction. Cross-sectional transmission electron microscopy (X-TEM) is used to obtain a microscopic view of the ion-beam modified C_{60} film. Atomic force microscopy (AFM) was used to image the disruption to the surface packing of the C_{60} molecules due to the ion impact.

EXPERIMENT

The C_{60} films were prepared by thermal evaporation of purified C_{60} powder kindly provided by Peng (CSIRO Division of Coal Research) onto Si substrates. Typical thicknesses were of the order of 350 nm as determined by surface profilometry. In order to minimize the effects of the differences of the properties of films produced in different deposition runs, the samples used for the FTIR, Raman, and AFM studies were all cut from a single deposited film. However, due to the fact that the thickness of the deposition was not uniform over the whole of the wafer, the thickness of the samples used for irradiation with different doses varied by up to ± 100 nm. For the TEM measurements C_{60} films were deposited on thinned glassy carbon wafers, which were then cut in cross section using an ultramicrotome, and imaged in a JEOL 2010 electron microscope operating at 200 keV.

Samples were subjected to Xe ion implantation at 620 keV ($R_p \pm \Delta R_p = 200 \pm 20$ nm) at room temperature. Thus the ion-beam modified layer constituted about half the thickness of the original film. The 620-keV energy was chosen as the spectroscopic diagnostics employed herein (FTIR and Raman spectroscopies) have skin depths comparable to the ion range. For one set of Raman measurements 320-keV irradiations were used (see Fig. 3) to allow a comparison to the previous conductivity measurements (see Ref. 6), but these were not used for the quantitative analysis. For the samples used for the FTIR, Raman, and AFM measurements, half of the sample was masked from the ion beam to serve as an unimplanted reference.

Raman measurements were performed in backscattering geometry using the 514-nm line of an Ar ion laser on a DILOR *XY* micro-Raman spectrometer. The laser beam was focused onto the sample using a $\times 100$ objective, thus providing a laser spot size about 2 μm in diameter. In order to avoid sample degradation during the measurements very low powers were employed (< 0.5 mW) and the sample was slowly scanned under the laser beam. Sample degradation due to laser damage could be identified by the observation of a rise in the background in the Raman spectrum as data were being collected. If this was seen to occur, the measurement was rejected and the run was repeated. In each case spectra were collected from both the implanted and unimplanted sides of each specimen.

Fourier-transform infrared measurements were performed in reflection mode on the same set of samples as were used for the Raman measurements. The FTIR measurements were performed on a Brukker IFS 88 FTIR spectrometer equipped with a microscope attachment. The MCT detector employed limited the frequency region which can be studied to 600–4000 cm^{-1}. All FTIR spectra were referenced to an uncoated Si substrate. The data were collected using a spectral resolution of 2 cm^{-1} and a scanner velocity of 0.85 cm/s. Noise reduction for

each spectrum was effected by averaging over 1000 scans. The IR microscope was employed in reflection mode with a magnification of ×15 and an aperture limiting the diameter of the collection area to about 250 μm. Several measurements were taken over different regions of the specimen and the results presented here are averages of these measurements. Fourier-transform IR measurements were also performed in transmission mode, but these were found to suffer from interference from some of the underlying untransformed C_{60} material and have therefore not been used for the analysis below.

A Digital Instruments NanoScope III atomic force microscope (AFM) was used to image the structure of the unirradiated and irradiated C_{60} films. All images were obtained using microfabricated Si_3N_4 cantilevers (Digital Instruments) with a manufacturer's quoted spring constant of 0.58 N/m; however an independent calibration of these cantilevers found the spring constant to be 0.32±0.02 N/m. The AFM was operated in the constant deflection mode (i.e., the tip-sample distance was adjusted to maintain a constant force and hence constant deflection of the cantilever). The images reported herein were recorded in air at ambient conditions, with a scanning force of about 100 pN. In a typical measurement, the tip was brought into contact with the specimen surface, and the imaging force adjusted to the desired strength (usually between 100 and 300 pN). Images were then collected at scan rates of between 5 and 20 Hz, the speed being optimized to obtain the clearest images. Under these imaging conditions, the films appeared to be stable under the AFM probing. The reproducibility of the images was checked by changing parameters such as the scan size and direction while verifying that the visible structures altered accordingly. The most important parameter for obtaining reproducible images was found to be the imaging force which needed to be kept roughly constant in order to obtain similar images from different regions of the same sample. Images were taken of at least two different areas on each C_{60} sample, and representative images are presented here.

The horizontal scans were calibrated by imaging freshly cleaved mica at a resolution where the repeat unit cells of 5 oxygens were easily visible in the raw images. The nearest-neighbor center-center separations of these unit cells are well defined and were used as the calibration distances. The lateral resolution was adequate to reveal the packing of the C_{60} molecules on the surface but was not sufficient to be able to resolve the individual C atoms within the fullerene molecule.

RESULTS

The results of the FTIR measurements for unimplanted C_{60} and for the most heavily implanted (3.2×10^{12} and 1×10^{13} Xe/cm²) samples are shown in Fig. 1. For clarity of presentation, vertical offsets of −0.03 and +0.02 have been applied to the data for the 3.2×10^{12} Xe/cm² and 1×10^{13} Xe/cm² samples, respectively. Once these offsets are taken into account it is evident that the dependence of the continuum on wave number for the 3.2×10^{12} Xe/cm² sample follows closely the dependence
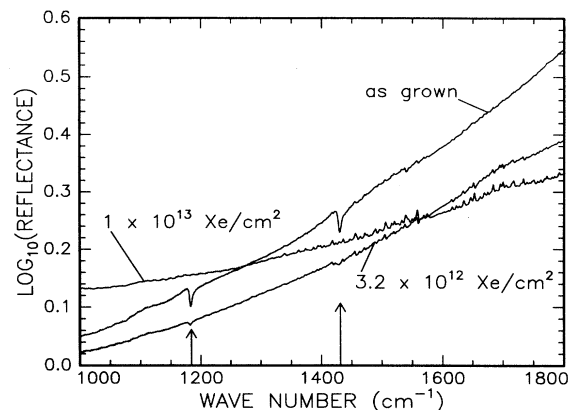

FIG. 1. Fourier-transform infrared spectrum of as-grown C_{60} films, together with the spectra for films irradiated with 3.2×10^{12} and 1×10^{13} Xe/cm² (620 keV). The arrows indicate the C_{60} IR absorption bands at 1183 and 1430 cm⁻¹. For clarity of presentation, vertical offsets of −0.03 and +0.02 have been applied to the data for the 3.2×10^{12} and 1×10^{13} Xe/cm² samples, respectively.

for the virgin C_{60} film. However, it is also clear that the dependence of the continuum on wave number for the 1×10^{13} Xe/cm² sample is different to that of the virgin material. This may be due to the presence of a significant amount of amorphous carbon in the film at these high doses which changes the overall surface reflectivity.

As indicated by arrows in Fig. 1 the dominant peaks in the as-deposited specimen are at 1183 and 1430 cm⁻¹. These peaks are due to vibrations of C atoms which are predominantly tangential to the surface of the fullerene sphere.[7] Peaks due to water vapor are also evident in the spectrum, especially in the region between 1400 and 1800 cm⁻¹. The origin of these peaks is most likely from the residual water vapor in the space located between the objective of the IR microscope and the sample.

It is clear that the peaks due to the presence of C_{60} are severely attenuated for a dose of 3.2×10^{12} Xe/cm² and have completely vanished for the highest dose of 1×10^{13} Xe/cm². Careful examination of the spectrum at these and lower doses failed to reveal any additional peaks which may have been attributed to fullerene fragments.

For quantitative analysis, the peak at 1180 cm⁻¹ was chosen as this region of the spectrum is free of peaks due to contamination by water vapor. The decrease in the intensity of the 1180-cm⁻¹ peak with increasing dose is shown in Fig. 2, after subtraction of the background. It should be noted that the only effect of the ion irradiation is a decrease in peak intensity, without any noticeable change in peak position or width, except perhaps a very slight downward shift in energy at the very highest doses.

Figure 3 depicts the Raman spectra of unirradiated C_{60}. The peaks observed are consistent with those previously reported[7] and have been attributed to the internal modes of the C_{60} molecule. The spectrum is dominated by the A_g peak at 495 cm⁻¹ which corresponds to a radial breathing mode and by a peak at 1467 cm⁻¹ which
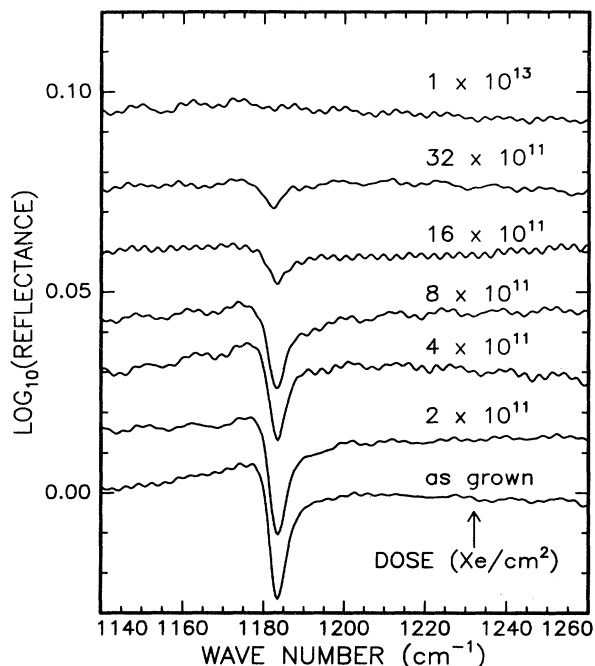
FIG. 2. The diminution of the 1183-cm^{-1} IR band as a function of Xe ion dose (620 keV), after subtraction of the sloping background. Note that the diminution of the peak is not accompanied by shifts in the peak position or by line broadening or skewing. The oscillations observed in some of the spectra are due to interference attributable to internal reflections in the films.
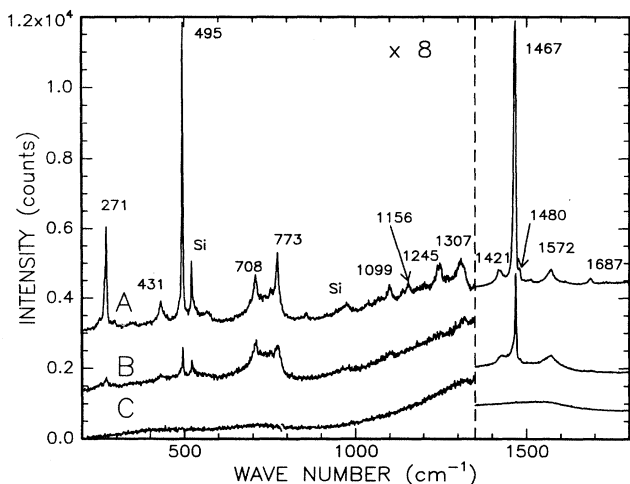
corresponds to a breathing mode in which the 5 C atoms are tangentially displaced around the pentagons.[7] Figure 3 also shows the spectra from samples irradiated with 1×10^{13} and 1×10^{14} Xe/cm^2 (320 keV). The attenuation of the peaks corresponding to the diminution of the number of intact C$_{60}$ spheres is evident. Interestingly, the peaks at 708, 773, 1421, and 1572 cm^{-1} do not appear to be as sensitive to the ion-beam damage as the more intense peaks in the spectrum. We comment below on a possible reason for this. It is also interesting to note that the peaks due to Si disappear, which is an indication of the increased opacity of the film which covers the Si substrate. At the highest doses all of the peaks corresponding to C$_{60}$ have disappeared and the spectrum consists of a rather broad peak centered at about 1530 cm^{-1} which is typical of the Raman spectrum of amorphous carbon (a-C).

Figure 4 shows in greater detail the gradual diminution of the most intense C$_{60}$ peak at 1467 cm^{-1} as a function of ion dose, for samples irradiated with 620-keV Xe. Note that the peak at 1467 cm^{-1} does not shift or appreciably broaden over the range of doses examined. At the highest doses ($> 3.2 \times 10^{12}$ Xe/cm^2), a small shoulder does appear on the low wave-number side of the main 1467-cm^{-1} peak centered at about 1462–1465 cm^{-1}. Apart from this shoulder, no other new peaks were ob-

FIG. 3. Raman spectra of A, as grown C$_{60}$ film; B, C$_{60}$ irradiated with 1×10^{13} Xe/cm^2 (320 keV); and C, C$_{60}$ irradiated with 1×10^{14} Xe/cm^2 (320 keV). The spectra have been offset in the vertical direction for clarity of presentation. Note that no new peaks which would indicate the presence of fullerene fragments are observed in the spectra. Similar spectra are obtained for irradiation with 620-keV Xe ions.
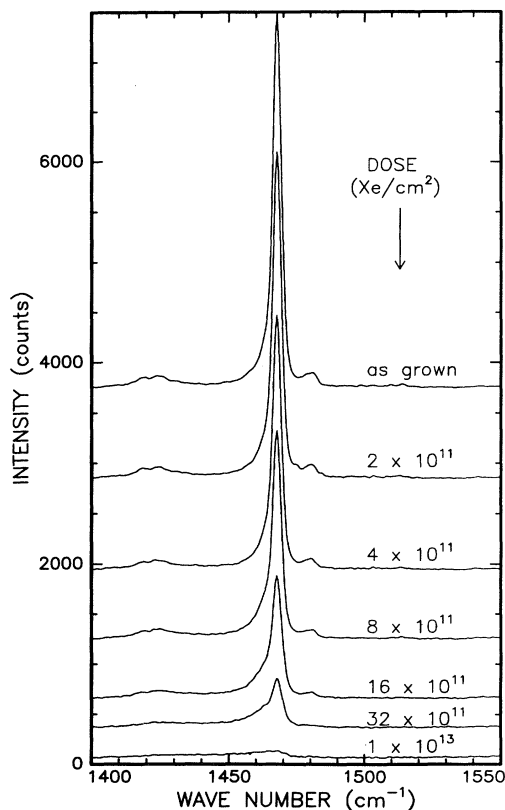

FIG. 4. The diminution of the 1467-cm^{-1} C$_{60}$ Raman band as a function of Xe ion dose (620 keV). Note that the diminution is not accompanied by shifts in the peak position or by line broadening or skewing.
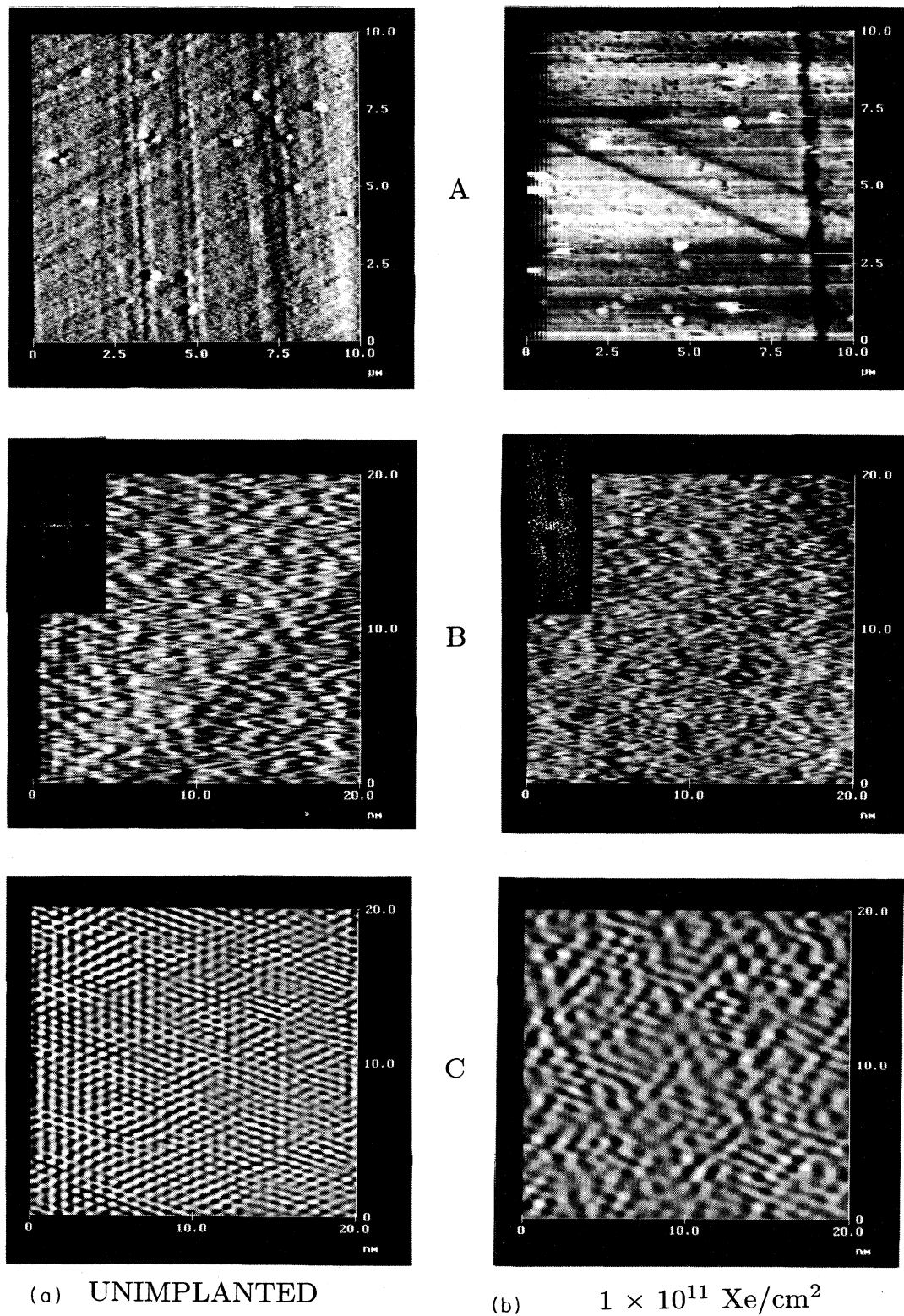
(a) UNIMPLANTED   (b) 1×10^{11} Xe/cm^2

FIG. 5. Atomic force microscope images of (a) unimplanted C$_{60}$ films and (b) a C$_{60}$ film irradiated with a dose of 1×10^{11} Xe/cm^2 (620 keV). In each series A shows a "raw" image of a 10×10 μm^2 area of the film; B shows a "raw" image of a 20×20 nm^2 area; and C shows the images in B after filtering of high-frequency noise using a 2D fast Fourier transform. The inset in B is the 2D FFT of the raw data used to filter images which are displayed in C.

served following the ion-beam irradiation.

Cross-sectional TEM was performed on the various implanted C_{60} films. Because of the absence of Z contrast (since all the materials are predominantly composed of carbon), it was necessary to use a large negative defect of focus in order to enhance the contrast, but even so attaining high-quality micrographs proved to be difficult. From the cross-sectional micrographs it was possible to observe that at high doses the ion beam amorphizes the C_{60} films; an observation in agreement with the Raman measurements. It was also evident from the micrographs that the irradiated films were significantly thinner than the unirradiated material. At the doses and beam energies employed, significant material loss due to sputtering is most unlikely. Thus we conclude that the decrease in the thickness is probably due to a compaction (i.e., densification) of the film following the ion irradiation. In addition, for doses exceeding 1×10^{12} Xe/cm^2, the surface of the film displays increased roughness as compared to the lower dose specimens. To confirm the compaction of the material following ion-beam irradiation measurements of the areal density using Rutherford backscattering spectroscopy (RBS) coupled with step height measurements would be desirable; however, such measurements will have to be undertaken with caution as it is likely that the He probing beam used for RBS will itself modify and compact the material.

The results of atomic force microscopy measurements of an unimplanted portion of a C_{60} sample are compared with those obtained under identical conditions for the part of the sample which has been irradiated with a very low dose of Xe $(1 \times 10^{11}$ $Xe/cm^2)$ in Figs. 5(a) and 5(b), respectively. Displayed are A, the raw data taken at a low magnification showing a scan over a 10 $\mu m \times 10$ μm area; B similar raw data taken at a higher magnification covering an area of 20 nm $\times$ 20 nm; and C the same 20 nm $\times$ 20 nm images after filtering of high-frequency noise using a two-dimensional (2D) fast Fourier transform (FFT). The FFT spectra of the raw data are shown as insets to the images displayed in B. The FFT for the unirradiated specimen shows an array of bright spots corresponding to a hexagonal ordering with a lattice spacing of about 0.8 nm. By contrast, the FFT of the irradiated material shows a disordered array of spots indicating a high level of disorder which is also evident in the filtered images shown in C. It is important to note that the images in Figs. 5(a) and 5(b) are displayed using the same contrast settings and that exactly the same filtering has been applied to the raw image in B for both the unimplanted [Fig. 5(a)] and implanted [Fig. 5(b)] cases. Figure 5 demonstrates that even at extremely low doses, the ion beam has destroyed the surface ordering. Similar disruption to the surface order was also seen in the specimens irradiated at higher doses.

DISCUSSION

The absence of new peaks in the Raman and FTIR spectra and the lack of any observed peak shifts is strong evidence that no intermediate fragments of C_{60} in any substantial amounts are being created as a result of the ion irradiation. This is in contrast to the results of lower energy ion impact and other energy deposition mechanisms.[8] For example, for 50-eV C ion impact on C_{60}, a series of C_2 loss fragments such as C_{58}, C_{56}, C_{54}, etc., can be observed, as is also the case when C_{60} is photodissociated.[9] On the other hand, at very low energies, or when He is used instead of C, new signals appear at higher masses than C_{60}.[8] For He irradiation it is thought that He is actually incorporated inside the cage.

The Raman and FTIR spectra of such fullerene fragments have not been reported. However, it is reasonable to assume that the peaks from such fragments would be expected to appear in the spectral region which we have investigated in this study. This assumption is reasonable because the C-C bond length in such fragments would not be expected to be very different from that in graphite, and thus the vibrational frequencies would be expected to be comparable to those observed in a wide range of sp^2 bonded C materials, all of which display the majority of their Raman and IR active modes below 1600 cm^{-1} which is the cutoff frequency in the density of states of graphite. Examination of the vibrational spectra of "modified" fullerenes, such as C_{70} and alkali doped fullerenes[7] lend further support to the proposition that most of the important modes appear in the range below 1600 cm^{-1} which we have examined closely in this study. Thus we conclude that the absence of new peaks in the region 400–1600 cm^{-1} is strong evidence for the absence of any fullerene fragments following the ion-beam irradiation.

Recently, it has been reported that laser irradiation of C_{60} films results in downward shifts in the main Raman peak from 1469 to 1458 cm^{-1} and in the emergence of many new peaks in both the Raman and FTIR spectra.[10] These observations were interpreted as being attributable to the photoinduced dimerization and polymerization of C_{60}. In the present work, there is some evidence of a shoulder emerging for the highest dose irradiations at 1460–1465 cm^{-1}, but no new other peaks, such as were reported for the case of the laser-induced polymerization,[10] were observed in the present work. We comment on the possible origin of this shoulder below.

In our previous work,[6] which was based on measurements of the ion-beam-induced conductivity of C_{60} films, we showed that the conducting species released by the ion impact were individual C atoms. The conductivity is expected to be governed by the largest available conducting centers, and hence the observation that the conducting species are C atoms is also strong supporting evidence that upon high-energy ion impact each fullerene molecule completely decomposes into its constituent atoms in a single catastrophic event, in contrast with the results of other energy deposition processes for which it was found that the fullerene molecule decomposed into smaller clusters of carbon atoms.[9]

The cross section for the destruction of the C_{60} molecules can be obtained from the decrease in the Raman and FTIR peak intensities as a function of ion dose as shown in Figs. 2 and 4. Following the analysis suggested in Ref. 5 we assume that the areal density, N, of the ful-

lerene molecules remaining after irradiation with an ion dose, D, is given by

$$N = N_0 e^{(-\sigma D)} , \qquad (1)$$

where σ is the cross section.

For the FTIR measurements N is proportional to the $\log_{10}$ (reflectance) (which is the parameter which has been plotted in Figs. 1 and 2). For the Raman measurements, N is proportional to the integrated Raman intensity. Hence, for the Raman measurements a plot of $\log_{10}[I(D)/I_0]$ vs dose where $I(D)$ is the intensity of a particular Raman peak after a dose D, and I_0 is the intensity of the corresponding peak in the unirradiated film, should yield a straight line whose slope is the cross section, σ, for destruction of C_{60} by the ion beam. A similar analysis should also be possible using the intensity of the FTIR peaks, where the $\log_{10}$ (reflectance) is used to determine the intensity of the absorption due to a particular mode.

In Fig. 6, the intensity of the 1183-cm^{-1} IR absorption band after a given ion dose, $I(D)$, is plotted as $\log_{10}[I(D)/I_0]$ vs dose [i.e., $\log_{10}$ (normalized peak intensity) vs dose]. Similarly, in Fig. 7, the intensity of the Raman band at 1467 cm^{-1} after a given dose, $I(D)$, normalized to the intensity of this peak for the unirradiated material, I_0, is plotted as $\log_{10}[I(D)/I_0]$ vs dose. The Raman and FTIR data when plotted in this way do indeed follow a straight-line dependence although the linear fit is better for the Raman than the FTIR measurements. The linear fits to the Raman data in Fig. 7 yield a cross section of $\sigma = 7.3 \pm 1.8 \times 10^{-13}$ cm^2 from the Raman data while $\sigma = 4.6 \pm 1.1 \times 10^{-13}$ cm^2 is deduced from the FTIR data in Fig. 6. The errors have been estimated on the basis of lines of worst fit taking into account the uncertainties in each of the data points.

The cross section as measured by infrared spectroscopy is somewhat lower than that obtained from the Raman measurements. We speculate that this difference, if significant, may be connected with another observation made above, viz., that the weaker peaks in the Raman spectrum (see Fig. 3) decay more slowly as a function of
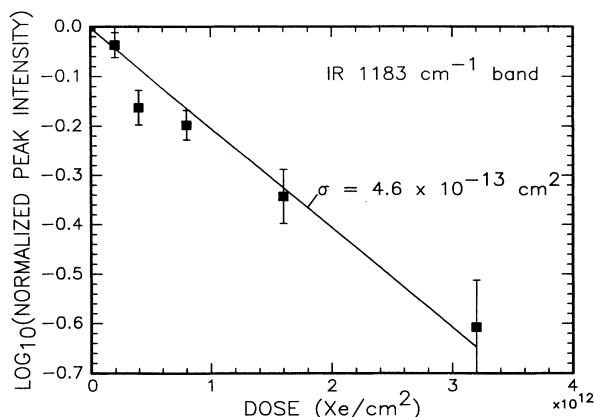
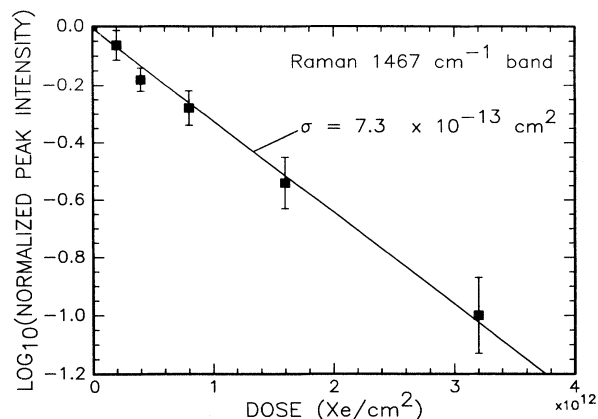

FIG. 7. The diminution of the intensity of the 1467-cm^{-1} Raman band as a function of Xe (620-keV) ion dose displayed as $\log_{10}[I(D)/I_0]$ vs dose.

dose than the strong Raman lines. It is possible that the two strongest peaks in the Raman spectrum (which originate from highly symmetric A_g modes of vibration) are particularly sensitive to the lowering of symmetry of the C_{60} molecule which results from the interaction of intact C_{60} molecules with the isolated carbon atoms produced by the destruction of other C_{60} molecules. This would result in a change in the relative intensities of the Raman lines with increasing ion dose because the weak lines (corresponding to lower symmetry modes) would decay in response to the loss of C_{60} alone, whereas the strong lines, while being primarily sensitive to the loss of C_{60}, would also diminish due to the formation of C_{60}-C complexes.

As stated in the Introduction two different mechanisms have been proposed for the ion-beam-induced disintegration of C_{60}. The first, based on an examination of the response of C_{60} films to proton irradiation[5] suggested that the energy deposited by the ion due electronic stopping processes is responsible for the destruction of the C_{60}, whereas the data based on Xe irradiation[6] indicated that the energy deposited in elastic nuclear collisions is the cause of the C_{60} modification. A comparison between the cross section determined here (σ_{Xe}) to that previously obtained for proton irradiation (σ_H) allows the discrimination between these two mechanisms in the following way. From the Monte Carlo computer code TRIM,[11] it is possible to obtain an estimate of $(dE/dx)_{electronic}$ and $(dE/dx)_{nuclear}$ for both 200-keV protons and 620-keV Xe ions slowing down in a carbon-based material having the macroscopic density of C_{60}. These ratios are found to be

$$(dE/dx)_{nuclear}(Xe)/(dE/dx)_{nuclear}(H) = 1.6 \times 10^4$$

and

$$(dE/dx)_{electronic}(Xe)/(dE/dx)_{electronic}(H) = 18.5 .$$

In other words, if the electronic energy deposited in the film is primarily responsible for the ion-beam-induced transformation, the cross section for 620-keV Xe should be only about 18 times higher than for 200-keV H,

FIG. 6. The diminution of the intensity of the 1183-cm^{-1} IR absorption band as a function of Xe (620 keV) ion dose displayed as $\log_{10}[I(D)/I_0]$ vs dose.

whereas if nuclear stopping is responsible this ratio should be 1.6×10^4. In fact, using $\sigma_H = 6.1 \times 10^{-17}$ cm^2 as determined for 200-keV protons,[5] and $\sigma(\text{Xe}) = 6 \times 10^{-13}$ cm^2 as found here from the average of the cross sections as determined by the Raman and IR measurements, the experimentally determined ratio of the cross sections is

$$\sigma(\text{Xe})/\sigma(\text{H}) = 1.0 \times 10^4 \ .$$

This ratio is in excellent agreement with that expected from TRIM (Ref. 11) for nuclear stopping (being 1.6×10^4) and is in sharp contrast with that expected for an electronic process (18.5). Thus the cross section for destruction of C$_{60}$ scales with $(dE/dx)_{\text{nuclear}}$ and not with $(dE/dx)_{\text{electronic}}$, and hence the present data clearly support the notion that it is the nuclear and not the electronic collision processes which are primarily responsible for the ion-beam-induced transformation of C$_{60}$.

We note that similarly good agreement with the experimentally determined ratio of cross sections can be obtained if one considers the ratios $(dE/dx)_{\text{total}}(\text{Xe})/(dE/dx)_{\text{nuclear}}(\text{H})$ or $(dE/dx)_{\text{electronic}}(\text{Xe})/(dE/dx)_{\text{nuclear}}(\text{H})$. This is because, coincidentally, for 620-keV Xe irradiation

$$(dE/dx)_{\text{nuclear}}(\text{Xe}) \simeq (dE/dx)_{\text{electrons}}(\text{Xe}) \ .$$

This observation, however, does not affect the conclusion reached above since in all cases it is $(dE/dx)_{\text{nuclear}}(\text{H})$ and not $(dE/dx)_{\text{electronic}}(\text{H})$ which appears in the denominator of the ratios, i.e., we can rule out a scaling based on electronic energy loss alone. We cannot, however, completely rule out the possibility that electronic processes play a secondary role in the transformation, and we comment on the possible role for $(dE/dx)_{\text{electronic}}(\text{Xe})$ below. What is clear is that the dominant driving force for the transformation is nuclear knock-on collisions.

The AFM measurements presented above illuminate another aspect of the ion-beam-induced transformation of C$_{60}$ films as this method is sensitive to the surface of the material under study. Whilst the FTIR and Raman measurements are sensitive to the internal vibrational modes within the C$_{60}$ molecule, the AFM images the way in which these molecules are arranged on the surface, i.e., AFM is sensitive to ordering of the C$_{60}$ molecular solid. Experimentally, the AFM measurements differ from the other measurements presented here in that they show dramatic change to the surface ordering to occur at doses as low as 1×10^{11} Xe/cm^2, whereas at this dose no significant changes can be detected using the other techniques employed in this study, nor in the electrical conductivity.[6] Thus a dose of 1×10^{11} Xe/cm^2 is sufficient to destroy the ordering of the surface of the fullerene "crystal" whereas the FTIR and Raman measurements show that most of the C$_{60}$ molecules are still intact at this dose.

A simple estimate of the probability that a C$_{60}$ molecule within the irradiated volume will be destroyed following a dose of 1×10^{11} Xe/cm^2 can be obtained by multiplying the ion dose by the cross section. Using the cross section of 6×10^{-13} cm^2 (as deduced from the Raman and

IR measurements) an estimate of about 6% for the fraction of C$_{60}$ molecules destroyed is obtained, i.e., in an area of 20×20 nm (as is shown in Fig. 5) one would expect about 30 of the roughly 500 C$_{60}$ clusters within this imaged area to be destroyed for the above dose. Another view of this is that the effective radius for destruction of the C$_{60}$ molecule, r, is given by $\pi r^2 = \sigma$, or $r = 4.4$ nm for $\sigma = 6 \times 10^{-13}$ cm^2. This is about 12 times the geometric size of the C$_{60}$ molecule. The reason for this large effective radius is that the experimentally determined cross section measures not only the primary knock-on event but also the effect of "knocked-on" C atoms destroying C$_{60}$ molecules in the collision cascade.

However, even this relatively large effective radius is not adequate to describe the data shown in Fig. 5 which shows the complete loss of the surface structure following a dose as low as 1×10^{11} Xe/cm^2 in an area of 20×20 nm.

The data of Fig. 5, can, however, be understood by considering that it is the destruction of C$_{60}$ molecules throughout the entire thickness of the film which is reflected in surface roughness caused by C$_{60}$ spheres "falling in" to fill the gaps left by the missing spheres. The picture is akin to a box filled with balloons stacked in an ordered fashion such that the surface is smooth. If, however, some of the balloons are allowed to explode at random throughout the volume, the rearrangement of the remaining balloons leads to a roughened surface. This is exactly what the AFM data show.

It is noteworthy that C$_{60}$ appears to show this surface roughening at doses much lower than those required to produce similar effects in other sp^2 bonded carbons.[12] A reason for this may be as follows. The C$_{60}$ lattice is only weakly bonded by van der Waals forces, and the binding energy of the lattice is small as compared to the binding energy of the molecule itself. The AFM records the amorphization of the lattice of C$_{60}$ molecules, while most of the molecules themselves remain intact at very low doses. The source of the energy that disrupts the crystal lattice may be the thermal spike which accompanies the passage of the ion through the solid. This spike is initiated during the nuclear knock on of a carbon atom. However, the molecule or atom is left in an excited state, and this energy is dissipated in low-energy interactions over ps time intervals, and radiates outwards from the center of the nuclear collision. In most crystals, most of this phonon-type energy can be absorbed without creating permanent lattice disruption. However, in a weakly bonded solid such as C$_{60}$ the energy contained in the thermal spike even far away from its point of origin in a knock-on event may be sufficient to disrupt the lattice, although not sufficient to break up the C$_{60}$ molecule itself.

Finally we offer a speculation about the emergence of a shoulder on the low wave-number side of the main 1467-cm^{-1} Raman peak. We have established that the break up of the C$_{60}$ clusters depend primarily on the nuclear energy deposited in the irradiated volume. Nevertheless, it should be recalled that about half the energy of a 620-keV Xe ion is in fact lost in inelastic electronic collisions. From TRIM,[11] for 620-keV Xe ions,

$$(dE/dx)_{\text{electronic}}/(dE/dx)_{\text{nuclear}} = 1.18 \ .$$

keV Xe ion is in fact lost in inelastic electronic collisions. From TRIM,[11] for 620-keV Xe ions,

$$(dE/dx)_{electronic}/(dE/dx)_{nuclear} = 1.18 .$$

Recently it has been shown that electron stimulated polymerization of C_{60} is possible.[13] Therefore we speculate that a small fraction of the C_{60} molecules may have undergone polymerization induced by the electron energy deposited by the ion as it passes through the film. Such polymerized C_{60} molecules are expected to show Raman peaks at somewhat lower energies than the main 1467-cm^{-1} peak,[10] and this may be the origin of the low wavenumber shoulder observed in the present work. However, the number of such polymerized chains would be expected to be small, as polymerization, if it occurs, will compete with the destruction of the C_{60} molecules induced by the nuclear energy deposited in the films. This may explain why the only "evidence" of polymerization is a small shoulder and no other new Raman peaks are observed.

CONCLUSION

The ion-beam modifications induced in fullerene films following ion-beam irradiation with 620-keV Xe ions have been investigated. The conclusions of this work regarding the ion-beam fullerene interaction and the nature of the material following ion irradiation are as follows.

(1) Each C_{60} molecule is destroyed in a single event; no smaller fullerene clusters can be detected.

(2) The process by which this destruction occurs depends primarily on the nuclear energy deposited in the irradiated volume and not on the electronic energy as proposed in Ref. 5. In other words, the destruction of the C_{60} molecule occurs via a direct knock-out event by either the impinging ion or by an energetic secondary knock-on C atom within the damage cascade.

(3) The cross section for the destruction of C_{60} molecules due to a collision with a 620-keV Xe ion (including the effect of secondary C recoils) was found to be $\sigma = 6 \pm 1.5 \times 10^{-13}$ cm^2 as deduced from Raman scattering and IR measurements.

(4) Atomic force microscopy measurements show that the surface packing of the C_{60} molecules is easily disrupted even at extremely low doses ($< 1 \times 10^{11}$ Xe/cm^2). The fact that this surface roughening occurs at such low doses may be connected with the weak van der Waals forces which bind the molecules together in the molecular solid.

Note added in proof. The conclusion that the destruction of C_{60} clusters is due to nuclear, rather than electronic processes has also recently been reported by J. Kastner, H. Kuzmany, and L. Palmetshofer, Appl. Phys. Lett. **65**, 543 (1994).

[1]H. W. Kroto, J. R. Heath, S. C. O'Brien, R. F. Curl, and R. E. Smalley, Nature **318**, 162 (1985).

[2]R. C. Haddon, Acc. Chem. Res. **25**, 127 (1992).

[3]P. W. Stephens, L. Mihaly, P. L. Lee, R. L. Whetten, S. M. Huang, R. Kaner, F. Diederich, and K. Holczer, Nature **351**, 632 (1991).

[4]J. Kastner, H. Kuzmany, L. Palmetshofer, P. Bauer, and G. Stingeder, Nucl. Instrum. Methods Phys. Res. B **80/81**, 1456 (1993).

[5]R. G. Musket, R. A. Hawley-Fedder, and W. L. Bell, Radiat. Eff. **118**, 225 (1991).

[6]R. Kalish, A. Samoiloff, A. Hoffman, C. Uzan-Saguy, D. McCulloch, and S. Prawer, Phys. Rev. B **48**, 18 235 (1993).

[7]M. S. Dresselhaus, G. Dresselhaus, and P. C. Eklund, J. Mater. Res. **8**, 2054 (1993).

[8]D. M. Gruen, Nucl. Instrum. Methods Phys. Res. B **78**, 118 (1993).

[9]S. C. O'Brien, J. R. Heath, R. L. Curley, and R. E. Smalley, J. Chem. Phys. **88**, 220 (1988).

[10]A. M. Rao, P. Zhou, K-A. Wang, G. T. Hager, J. M. Holden, Y. Wang, W. T. Lee, X. X. Bi, P. C. Eklund, D. S. Cornett, M. A. Duncan, and I. J. Amster, Science **259**, 955 (1993).

[11]J. F. Ziegler, J. P. Biersack, and U. Littmark, *The Stopping and Range of Ions in Solids* (Pergamon, New York, 1985).

[12]T. Li, B. V. King, R. J. McDonald, G. F. Cotterill, D. J. O'Connor, and Q. Yang, Surf. Sci. **312**, 399 (1994).

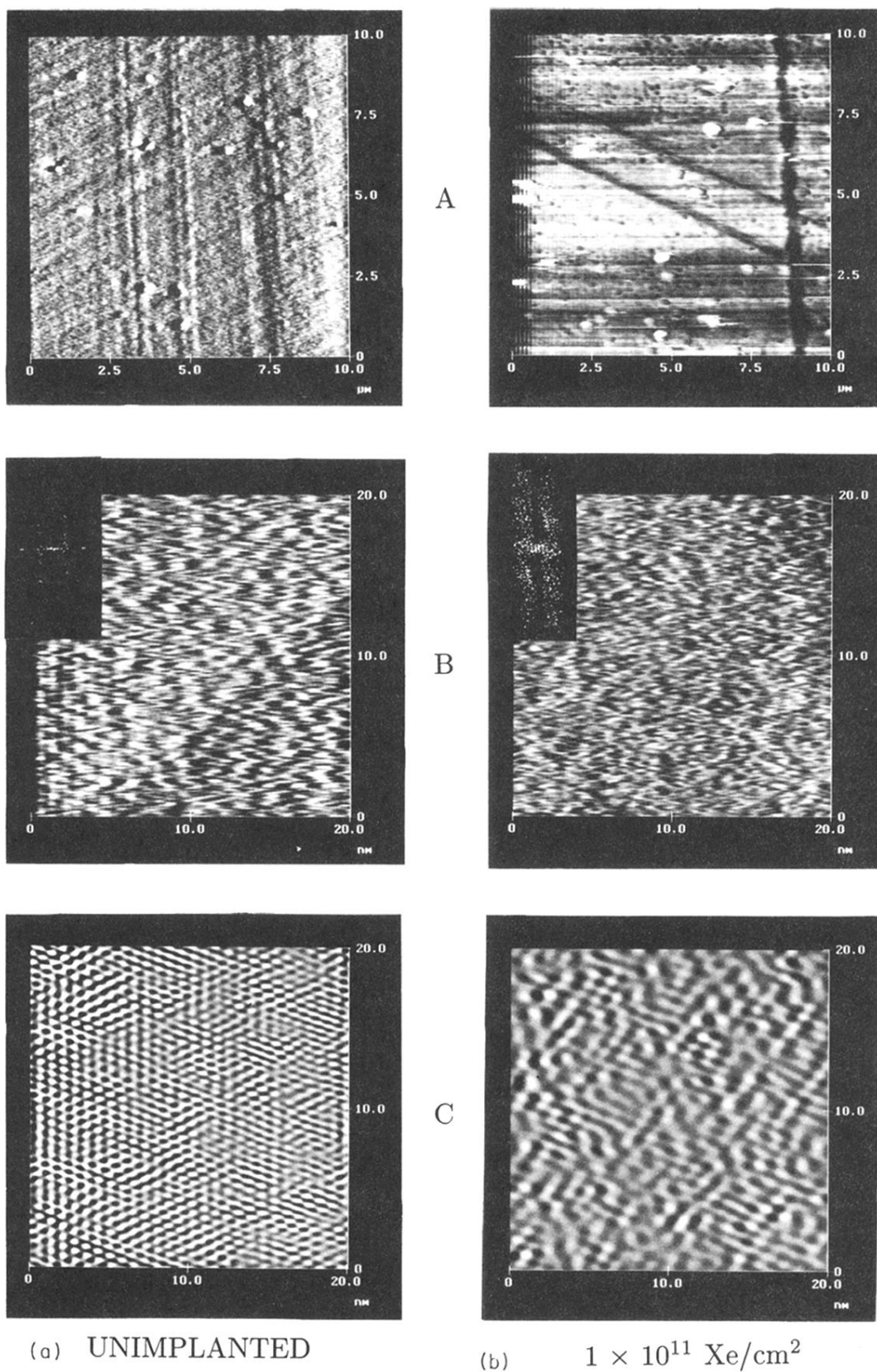[13]Y. B. Zhao, D. M. Poirier, R. J. Pechman, and J. H. Weaver, Appl. Phys. Lett. **64**, 577 (1994).

(a) UNIMPLANTED   (b) 1×10^{11} Xe/cm^2

FIG. 5. Atomic force microscope images of (a) unimplanted C$_{60}$ films and (b) a C$_{60}$ film irradiated with a dose of 1×10^{11} Xe/cm^2 (620 keV). In each series A shows a "raw" image of a 10×10 μm^2 area of the film; B shows a "raw" image of a 20×20 nm^2 area; and C shows the images in B after filtering of high-frequency noise using a 2D fast Fourier transform. The inset in B is the 2D FFT of the raw data used to filter images which are displayed in C.